Steady State Multiplicity of Adiabatic Gas-Liquid Reactors:

II. The Two Consecutive Reactions Case

SHANMUK SHARMA
LEE A. HOFFMAN
and
DAN LUSS

Department of Chemical Engineering
University of Houston
Houston, Texas 77004

A model describing two consecutive gas-liquid reactors in a continuously stirred-tank reactor is developed with reaction factors used to account for the interactions between the chemical and transport rate processes. A parametric numerical study revealed several interesting effects, including the existence of up to seven steady state solutions. The predictions of the model adequately describe the steady state multiplicity observed during the chlorination of liquid *n*-decane. It is shown that the steady state multiplicity can serve as an excellent tool for discriminating among rival models and estimation of kinetic parameters.

SCOPE

When gas-liquid reactions are carried out in a continuously stirred-tank reactor (CSTR), multiple steady states may exist as demonstrated by Ding et al. (1974). A detailed stability analysis of these multiplicities was presented by Schmitz and Amundson (1963 *a* to *d*) assuming that the overall reaction rate can be accounted for by a series chemical and mass transfer resistance model. Unfortunately, this series resistance model does not properly account for the mutual interaction between the chemical and transport rate processes in gas-liquid reacting systems, except when the mass transfer resistance is negligible.

One way of describing the overall rate of gas liquid reactions over a wide range of temperature, in which the controlling resistance shifts from kinetic to mass transfer, is by use of reaction factors (Teramoto et al., 1969). This method was used in a previous paper (Hoffman et al., 1975) in which we analyzed the steady state multiplicity of an adiabatic CSTR in which a single gas-liquid reaction occurred. It was found that the interaction among the chemical reaction, the transport resistances, and the solubility may cause the occurrence of up to five steady states. This is a rather unique feature of a gas-liquid reaction, as no more than three solutions can be attained when the same second-order reaction is carried out in a single phase CSTR.

In many industrial processes, for example, chlorination and hydrogenation, the reaction network consists of several gas-liquid consecutive-competitive reactions. One aim of this work is to develop a model of a CSTR in which two exothermic consecutive gas-liquid reactions occur and to test the validity of the model and the associated assumptions by comparing its predictions with experimental results. Another goal is to determine the parametric sensitivity and behavioral features of the system, and in particular examine the various multiplicity patterns and the maximal number of steady state solutions. This information is essential for the rational design, operation, and control of these gas-liquid reactors.

CONCLUSIONS AND SIGNIFICANCE

A model of a CSTR, in which two exothermic consecutive competitive gas-liquid reactions occur, has been developed with reaction factors used to account for the reaction in both bulk and film liquid (Teramoto et al., 1969). These factors are computed from Equations (15) to (17) and require the iterative solution of Equations (19) to (21). The steady state solutions can be determined from the intersections of the heat generation and removal graphs, and an efficient numerical procedure for computing these graphs is presented.

The capability of the model to describe real systems was tested by comparing its predictions with experimental data obtained by Ding et al. (1974) for the chlorination of *n*-decane. The comparisons, some of which are shown in Figures 1 and 2, indicate that the model adequately describes the experimental data when the formation of tri and higher chlorodecanes is small.

Numerical simulations revealed that changes in certain parameters can change both the nature of the multiplicity as well as the range of liquid residence time for which multiplicity exists. For example, Figure 3 describes a case for which changes in the reactivity of the *n*-decane can cause the appearance or disappearance of a special multiplicity pattern (an isola) for which a shift from the low to the high temperature steady state cannot be attained by increasing the residence time. The key parameters which influenced the multiplicity pattern and region were the kinetic rate constants, the interfacial area, the heat of the reactions, the heat loss from the reactor, and the liquid heat capacity. The simulations sug-

Correspondence concerning this paper should be addressed to Dan Luss. Shanmuk Sharma is with The M. W. Kellogg Company, Houston, Texas. Lee A. Hoffman is with Continental Oil Company, Ponca City, Oklahoma.

gest that the information about the multiplicity pattern and the ignition and extinction points can serve as an excellent tool for discriminating among rival models and assumptions and for the estimation of kinetic parameters.

The model predicts the occurrence of up to seven steady state solutions under certain operating conditions, and an example of such a case is shown in Figure 5. This occurrence of seven steady state solutions is a unique feature of gas-liquid reactors, as no more than five solutions can be attained in a homogeneous CSTR in which the same two consecutive second-order reactions are carried out.

In this work we examine the possible occurrence and implications of steady state multiplicity of a continuously stirred-tank reactor (CSTR) in which gas-liquid reactions occur. Specifically, we consider the following two consecutive gas-liquid reactions:

$$A(\text{gas}) + B(\text{liq}) \xrightarrow{k_1} R(\text{liq}) + L(\text{gas}) \qquad (1)$$

$$A(\text{gas}) + R(\text{liq}) \xrightarrow{k_2} S(\text{liq}) + L(\text{gas}) \qquad (2)$$

Second-order kinetics are assumed, as they adequately describe many gas-liquid reactions. The mathematical model is based on the following assumptions.

1. The temperatures of the gaseous and liquid feed streams are the same. The liquid feed does not contain any dissolved gas.
2. The temperatures of the gas and liquid inside the reactor are the same. The gas leaving the reactor is saturated with the liquid and passes through a condenser with a 100% efficiency. The condensate is returned continuously to the reactor.
3. The volumetric flow rate of the liquid leaving the reactor is independent of temperature and conversion.
4. The total pressure of gas bubbles is independent of position in the CSTR and of the operating temperature.
5. The mass transfer resistance in the bubbles is negligible.
6. The solubility of the gaseous reactant A in the liquid is independent of the conversion and its temperature dependence can be expressed as

$$\lg_{10}(x_A/P_A) = D_1/T - D_2 \qquad (3)$$

where x_A is the mole fraction of the dissolved A, and $P_A = y_A P$ is the corresponding partial pressure. Moreover, the solubility of the gaseous product L is negligible, and it is stripped from the liquid upon formation.

7. The heat of solution of the gas is independent of the temperature and composition of the liquid phase.

REACTION FACTORS AND THEIR COMPUTATIONS

When gas-liquid reactions are carried out in a CSTR, changes in the temperature can have a marked influence on the relative rates of the chemical and transport rate processes. While at low temperatures, the chemical reaction may be the rate limiting step; at higher temperatures, the overall rate may be controlled by the rate of mass transfer, and all the reactions may be completed in the mass transfer film. It should be noted that even when the reaction is controlled by mass transfer, the overall rate is often significantly larger than the maximal possible rate attainable by pure physical absorption. Consequently, a model which assumes that the overall rate is limited by a series of chemical and mass transfer resistances may lead to pitfalls when applied over a wide range of temperature. A model of the CSTR requires use of expressions which describe the rate of reaction in both the film and bulk liquid and which can account for the continuous shift from chemical to mass transfer control with increasing temperatures. One way of doing this is by use of reaction factors which are defined as

$$E_A^* \triangleq (R_A + F_l A_l/V_R)/(k_l a_v A_i) \qquad (4)$$

$$E_B^* \triangleq R_B/(k_l a_v A_i) \qquad (5)$$

$$E_R^* \triangleq R_R/(k_l a_v A_i) \qquad (6)$$

where $F_l A_l$ is the rate at which the gaseous reactant A leaves the reactor dissolved in the effluent liquid stream, and R_i denotes the rate of consumption or formation of species i per unit volume of reactor by reaction in both film and bulk liquid.

The reaction factors can be computed by any one of several models, for example, film model, surface renewal model, etc. For a single gas liquid reaction, the conversion of the liquid is rather insensitive to the model used in the computations. Calculations by Szekely and Bridgwater (1967) indicate that for a complex gas-liquid reaction network, the yield of the desired product may for certain kinetic parameters be somewhat sensitive to the model used. Because of the relative mathematical simplicity of the film model, we have used it in this work to compute the reaction factors. It should be noted that application of the film model to compute the reaction factor does not require computation of the mass transfer coefficient by that model.

The differential equations describing the reactions in the mass transfer film are

$$D_A \frac{d^2A}{dz^2} = k_1AB + k_2AR \qquad 0 < z < \delta \qquad (7)$$

$$D_B \frac{d^2B}{dz^2} = k_1AB \qquad 0 < z < \delta \qquad (8)$$

$$D_R \frac{d^2R}{dz^2} = -k_1AB + k_2AR \qquad 0 < z < \delta \qquad (9)$$

The corresponding boundary conditions are

$$A = A_i \qquad z = 0 \qquad (10)$$

$$\frac{dB}{dz} = \frac{dR}{dz} = 0 \qquad z = 0 \qquad (11)$$

$$B = B_l \qquad z = \delta \qquad (12)$$

$$R = R_l \qquad z = \delta \qquad (13)$$

$$-a_v D_A \frac{dA}{dz} = (k_1AB + k_2AR)(\epsilon - a_v\delta) + \epsilon A/\tau \qquad z = \delta \qquad (14)$$

Boundary condition (14) states that the rate of transfer of the dissolved gas to the bulk of the liquid is equal to the amount consumed by the reaction in the bulk plus that which leaves the reactor in the effluent stream. That

condition implicitly assumes that the concentration of the dissolved gas in the effluent stream is equal to the concentration of the gaseous reactant in the bulk fluid. This is a very good approximation for the practical cases in which the volume of the bulk fluid is significantly larger than that occupied by the mass transfer film. Boundary condition (11) is not strictly correct for a volatile liquid. However, accounting for the evaporation of the various liquid components and the return of the condensed vapor significantly complicates the analysis. Thus, the phenomenon is not accounted for in the determination of the reaction factor. A simple analysis of the influence of the evaporation of the liquid on the absorption rate for a system in which a single reaction occurs was presented by Pangarkar (1974).

An analytical solution of the above equations is not possible. However, an approximate solution was derived by Teramoto et al. (1969) applying the linearization technique of Van Krevelen and Hoftijzer (1948). Numerical computations indicate that the error introduced by this approximation is usually very small and of the order of several percents at most. According to Teramoto et al. (1969), the reaction factors are computed from the expressions

$$E_A^* = \frac{\gamma'}{\tanh \gamma'}\left(1 - \frac{a_l}{\cosh \gamma'}\right) \tag{15}$$

$$E_B^* = \frac{D_B B_l E_f}{D_A A_i \Gamma_A} + M^2(\alpha - 1)a_l \tag{16}$$

$$E_R^* = M^2(\alpha - 1)a_l\left(1 - \frac{1}{rs}\right) - \frac{D_R R_l E_f \Gamma_R}{D_A A_i \Gamma_A} \tag{17}$$

where we define

$$\begin{aligned} &\alpha = \epsilon/a_v\delta && M = \sqrt{(k_1 D_A B_l)}^{0.5}/k_l \\ &\gamma = M\sqrt{1 + 1/(sr)} && h = M\sqrt{D_A A_i/(D_B B_l)} \\ &r = D_B B_l/(D_R R_l) && s = k_l D_R/(k_2 D_B) \\ &\theta = k_l a_v \tau/\epsilon \end{aligned} \tag{18}$$

and

$$\gamma'^2 = M^2 b_i\left[1 + \frac{1/r + 1 - b_i}{1 + b_i(s - 1)}\right] \tag{19}$$

$$b_i = \frac{B_i}{B_l}$$

$$= \frac{1}{1 + h^2 \coth\gamma'/\gamma' - h^2/\gamma'^2 + h^2\gamma'(\sinh\gamma' - \gamma')/\bar{b}} \tag{20}$$

$$\bar{b} = \gamma'^2 \sinh\gamma'[\gamma' \cosh\gamma' + [\gamma^2(\alpha - 1) + 1/\theta]\sinh\gamma']$$

$$a_l = \frac{A_l}{A_i} = \frac{\gamma'}{\gamma' \cosh\gamma' + [\gamma^2(\alpha - 1) + 1/\theta]\sinh\gamma'} \tag{21}$$

$$E_f = \frac{\gamma'}{\tanh \gamma'}(1 + a_l)\left(1 - \frac{1}{\cosh \gamma'}\right) \tag{22}$$

$$r_i = \frac{R_i}{R_l} = s\, b_i[1 + r(1 - b_i)]/[1 + b_i(s - 1)] \tag{23}$$

$$\Gamma_A = \gamma'^2/(h^2 b_i) \tag{24}$$

$$\Gamma_R = \frac{r_i}{b_i s} - r \tag{25}$$

The computations of the reaction factors require iterative calculations. One starts by assuming a_l so that all the quantities defined by (18) can be computed. Subsequently, the coupled equations (19) and (20) are solved for b_i and γ', and the value of a_l is computed from (21) and compared with the assumed value. One then iterates until convergence between assumed and predicted values of a_l. The quantities defined by (22) to (25) are then computed and substituted into (15) to (17) to yield the reaction factors.

STEADY STATE EQUATIONS AND THEIR SOLUTION

Under steady state conditions, material and energy balances describing the CSTR are

$$q_{gf}y_{AF} - q_{go}y_A = R_A V_R + F_l A_l \triangleq k_l a_v V_R A_i E_A^* \tag{26}$$

$$q_{lf}x_{Bf} - q_{lo}x_B = R_B V_R \triangleq k_l a_v V_R A_i E_B^* \tag{27}$$

$$q_{lo}x_R - q_{lf}x_{Rf} = R_R V_R \triangleq k_l a_v V_R A_i E_R^* \tag{28}$$

where q_g and q_l are the gas and liquid molar flow rates, A_l is the bulk concentration of the dissolved gas, and the subscripts f and o refer to the streams entering and leaving the CSTR, respectively. In deriving (26), it is assumed that the concentration of the dissolved gaseous reactant in the effluent liquid stream is equal to its bulk concentration—A_l. This is an excellent approximation, since in a CSTR the volume of the bulk liquid is significantly larger than that occupied by the mass transfer film. The effluent liquid molar flow rate is equal to

$$q_{lo} = q_{lf} + F_l A_l \tag{29}$$

The interfacial concentration of the reacting gas can be expressed as

$$A_i = x_A \tilde{\rho}_l = x_A q_{lo}/F_l \tag{30}$$

where $\tilde{\rho}_l$ is the molar density of the liquid phase. Substitution of (29) into (30) yields

$$A_i = \frac{x_A q_{lf}}{F_l(1 - x_A a_l)} \tag{31}$$

where x_A can be computed from (3). The molar flow rate of the gas leaving the reactor and entering the condenser is equal to

$$q_{go} = (q_{gf} - F_l A_l)/(1 - y_B - y_R - y_S) \tag{32}$$

The molar flow rate of the gas leaving the condenser is

$$q_{gc} = q_{gf} - F_l A_l \tag{33}$$

where y_B, y_R, and y_S are the mole fractions of the evaporated liquid in the leaving bubbles, which are computed from thermodynamic vapor-liquid relations.

An energy balance on the CSTR yields

$$\begin{aligned} &R_B V_R(-\Delta H_1) + R_R V_R(-\Delta H_2) + F_l A_l(-\Delta H_l) \\ &\quad - q_{go}[y_B(-\Delta H_{vB}) + y_R(-\Delta H_{vR}) + y_S(-\Delta H_{vS})] \\ &\quad - Ua(T - T_c) - \int_{T_f}^{T} (q_{lo}c_{pl} + q_{gc}c_{pg})dT = 0 \end{aligned} \tag{34}$$

The steady state equations contain a large number of dependent and auxiliary variables. We present here a scheme of solving the equations and determining all the possible solutions.

Under steady state conditions, the number of gaseous reactant moles consumed by the reaction is equal to the number of moles of B reacted plus that of S formed. Therefore

$$R_A = R_B + (R_B - R_R) \tag{35}$$

Substitution of (35) into (26), (27), and (28) yields

$$x_B = (2q_{lf}x_{Bf} + q_{lf}x_{Rf} + q_{go}y_A + F_lA_l - q_{lo}x_R - q_{gf}y_{Af})/2q_{lo} \quad (36)$$

Equations (26), (27), and (28) can be rewritten as

$$y_A = (q_{gf}y_{Af} - a_vV_Rk_lA_iE_A^*)/q_{go} \quad (37)$$

$$x_R = (a_vV_Rk_lA_iE_R^* + q_{lf}x_{Rf})/q_{lo} \quad (38)$$

A material balance on component S yields

$$x_S = 1 - x_B - x_R - [F_lA_l + (1 - x_{Bf} - x_{Rf} - x_{Sf})q_{lf}]/q_{lo} \quad (39)$$

The above information about the mole fraction of the various components in the liquid phase can be used to compute the corresponding partial vapor pressures. Substitution of (4), (5), and (6) into the energy balance (34) and rearrangement yields

$$Q_I \triangleq a_vV_Rk_lA_iE_B^*(-\Delta H_1) + [a_vV_Rk_lA_i(E_A^* - E_B^*) - F_lA_l](-\Delta H_2) + F_lA_l(-\Delta H_s) = q_{go}[y_B(-\Delta H_{vB}) + y_R(-\Delta H_{vR}) + y_S(-\Delta H_{vS})] + Ua(T - T_c) + \int_{T_f}^{T}(q_{lo}c_{pl} + q_{gc}c_{pg})dT \triangleq Q_{II} \quad (40)$$

where Q_I and Q_{II} describe the energy generated and removed from the reactor, respectively. The above equation may be rewritten also as

$$Y_I \triangleq \frac{Q_I(T - T_f)}{Q_{II}} = T - T_f \triangleq Y_{II} \quad (41)$$

When the two Q or Y graphs are plotted as a function of the temperature, then any intersection between the graphs is a steady state solution. Thus, these graphs enable a systematic determination of all the possible steady state solutions.

The following numerical procedure was used by us successfully to determine the Q graphs. For a prescribed temperature and feed flow rates, we assume the values of y_A, x_R, and a_l and compute A_i and A_l from (3) and (31) and q_{lo} from (29). The values of x_B and q_{go} are determined simultaneously from (33), (36), and vapor-liquid equilibrium relations and used to compute

$$B_l = x_Bq_{lo}/F_l \quad (42)$$

Subsequently, we compute M from (18), and

$$R_l = x_Rq_{lo}/F_l \quad (43)$$

and solve (19) and (20) by Wegstein's method for b_i and γ', and determine a_l from (21). If the value of a_l does not agree with the assumed one, we iterate. After convergence, we compute E_f, r_i, Γ_A, and Γ_R from (22) to (25) and compute the reaction factors from (15) to (17). We then compare x_R from (38) with the assumed value and iterate. Finally, we compute y_A by (37) and if necessary iterate. The above information is sufficient for computing the Q values. This procedure was found to be rather efficient and rapid. Obviously, other iterative schemes could be developed for the calculations.

Every steady state is attained as a result of a start-up. Thus, it is of practical importance to determine which of the steady state solutions can be realized (stable) and which are unstable. (An unstable steady state is one for which any infinitesimal disturbance will move the reactor away from the steady state.)

A detailed discussion of the difficulties associated with a stability analysis of the model used here was presented by Hoffman et al. (1975). It was shown there that if one assumes that the reaction factors are still applicable, under transient conditions then any steady state which does not satisfy the slope condition

$$\frac{dQ_I}{dT} < \frac{dQ_{II}}{dT} \quad (44)$$

or equivalently

$$\frac{dY_I}{dT} < \frac{dY_{II}}{dT} = 1 \quad (45)$$

is unstable. The slope condition is only a necessary condition for stability. Thus, no general statement can be made on the stability of the solutions which satisfy this condition. We will not present a stability analysis of the system. All the unstable steady states which do not satisfy the slope condition are represented by a dashed curve in Figures 1 to 3 and also Figure 5.

NUMERICAL RESULTS AND DISCUSSION

Numerical simulations of the steady state model were carried out in order to test the capability of the model to describe the behavior of an experimental reactor, to check the parametric sensitivity of the model, to examine the behavioral features of the model and in particular the various multiplicity patterns and the maximal number of steady state solutions, and to explore the possible use of the multiplicity phenomenon as a tool to discriminate among rival models.

The capability of the model to describe real systems was tested by comparing its predictions with experimental results reported by Ding et al. (1974) on the chlorination of three lots of n-decane which had differing reactivities due to varying amounts of impurities. Figure 1 compares the predicted and observed data for the least active decane under conditions of constant gas feed rate. The dashed squares in Figure 1 describe the initial temperatures at which a shift to a high or low temperature steady state occurred. They approximate the temperatures of the intermediate unstable steady state solutions which cannot be realized without a proper control scheme. Table 1 reports the values of the parameters used in these simulations. A justification for the choice of parameter values can be found elsewhere (Hoffman, 1974). Figure 2 depicts the predicted and observed results for the same decane under conditions of equimolar gas and liquid feed rates. The ability of the model to adequately predict both types of experi-

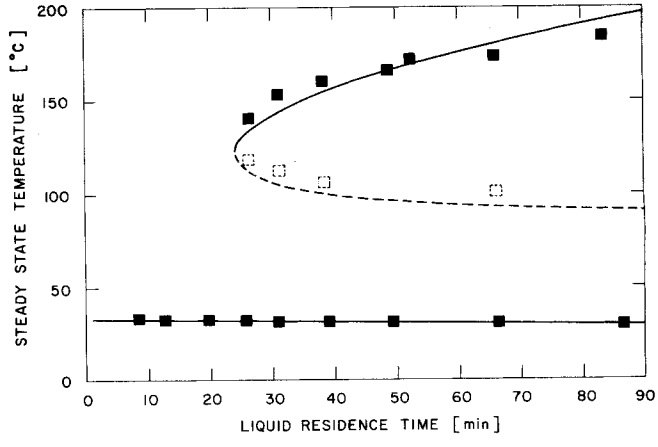

Fig. 1. Comparison of predictions of the model with experimental results on the influence of liquid residence time on the steady state temperature during the chlorination of n-decane with a fixed chlorine feed rate of q_{gf} = 2.8 g mole/hr.

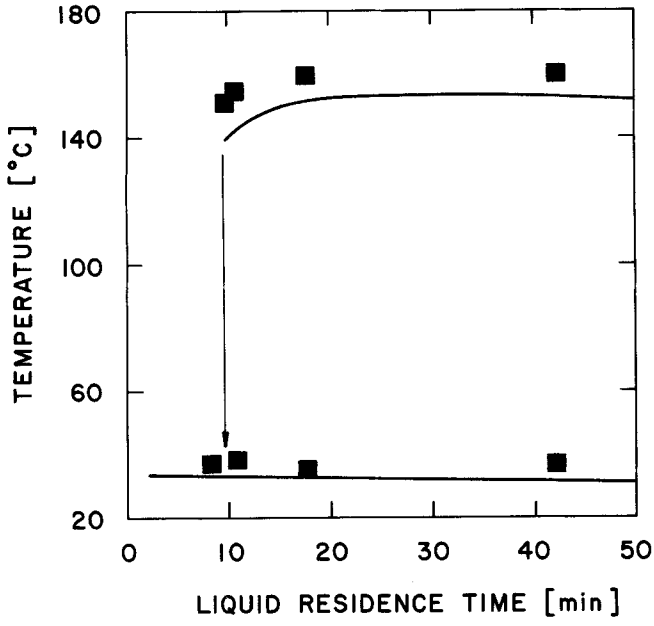

Fig. 2. Comparison of the predictions of the model with experimental results on the influence of liquid residence time on the steady state temperature during the chlorination of n-decane ($q_{lf} = q_{gf}$).

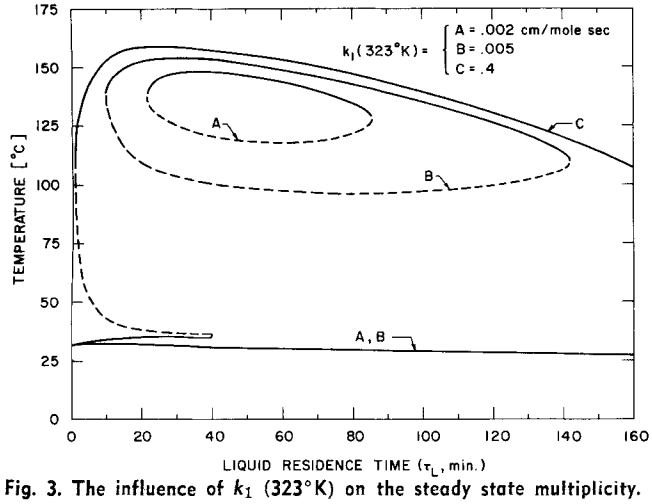

Fig. 3. The influence of k_1 (323°K) on the steady state multiplicity. Parameters reported in Table 1.

mental conditions was an indication of the validity of the model.

Data were also available for the more active decane lots. Experiments with the most active decane were performed under the same conditions as those for the least active decane (Table 1). Hence, the second test for the validity of the model was to compare its predictions against data for the most active decane by changing k_1 (323°K) only. [The values of the activation energies of the two reactions and k_1 (373°K)/k_2 (373°K) were assumed to be independent of the impurities.] A value of k_1 (323°K) = 1.7 cm³/mole-s simulated the experiments very well. All other parameters had the same values as reported in Table 1. The model properly predicted that for the more active *n*-decane lot a unique steady state exists for all τ_l. The maximal deviations between the measured and predicted temperatures and conversions for all these cases were 10°C and 5%, respectively.

The experiments with the moderately active decane were carried out with a different stirrer speed than those for the other *n*-decane lot. This caused a change in the liquid holdup and the transport coefficients. Therefore, simulations of the behavior of the CSTR with this decane required changing some of the parameters reported in Table 1.

Table 1. Parameters Used in the Simulation of the Experimental Results

$M_{WA} = 71$	$M_{WB} = 142$
$y_{Af} = 1.0$	$x_{Bf} = 1.0$
$\rho_{lf} = 0.725$ g/cm³	$P = 1$ atm
$T_f = 297$°K	$T_c = 298$°K
$Ua = 0.03$ cal/(°K-s)	$a_v = 3.0$ cm^{-1}
$\epsilon = 0.86$	$V_R = 400$ cm³
	$k_l = \sqrt{D_A}/0.1$ cm/s
$D_A = 0.66 \times 10^{-7} \exp 1\,172\left(\frac{1}{273} - \frac{1}{T}\right)$ cm²/s	
$D_B = 0.39\, D_A$	$D_R = .38\, D_A$
$C_{pA} = 8.28 + 5.6 \times 10^{-4}T$ cal/(mole °K)	
$C_{pL} = 6.7 + 8.4 \times 10^{-4}T$ cal/(mole °K)	
$C_{pl} = 4.25 + 0.234T$ cal/(mole °K)	
$C_{pg} = y_A C_{pA} + y_L C_{pL}$	
$\lg_{10}(x_A/y_A) = \frac{1\,010}{T} - 4.16$	
$P_B = 10^{[4.073 - 2702/(1.8T - 142)]}$ lb./sq.in.abs.	
$P_R = 10^{[4.343 - 3224/(1.8T - 134)]}$ lb./sq.in.abs.	
$P_S = 10^{[4.423 - 3462/(1.8T - 144)]}$ lb./sq.in.abs.	
$\Delta H_1 = -26\,000$ cal/mole	$\Delta H_2 = -27\,000$ cal/mole
$\Delta H_{vl} = -12\,000$ cal/mole	$\Delta H_s = -4\,500$ cal/mole
$\Delta E_1 = 29\,000$ cal/mole	$\Delta E_2 = 29\,000$ cal/mole
k_1 (323°K) = 0.005 cm³/(mole-s)	k_1 (373°K) = 1.414 k_2 (373°K)

The simulations revealed that the heat losses due to evaporation of the liquid were important factors, and a failure to properly account for them can induce a large error in the prediction of the high temperature steady states. The deviations between the predicted and measured temperatures and conversions of the high temperature steady states increased at high liquid residence time. These deviations were due to the fact that the model did not account for the formation of tri and higher chlorodecanes and their influence on the heat generation, the reaction factors, and the physical properties of the liquid.

Once the validity of the model was established, an extensive parametric sensitivity analysis of the model was performed by using an equimolar gas and liquid feed rate ($q_{gf} = q_{lf}$). A detailed report of the numerical simulations was presented by Hoffman (1974). This study revealed that the key factors which influence the reactor are the rate constants k_1 and k_2, the activation energies, the interfacial area, the heat of reactions, the heat losses, and the heat capacities. The effect of changing k_1(323°K) while holding all other parameters at the values reported in Table 1 is shown in Figure 3. The simulations indicate that changes of k_1 have a twofold impact. They affect the range of τ_l for which multiplicity exists and also change the nature of the multiplicity. The second effect was indeed surprising. For $k_1 = 0.4$ (curve C), the regular multiplicity pattern is obtained with both an extinction and an ignition. However, when the activity is reduced (curves B and A), a special multiplicity pattern, defined as an isola, is obtained. Here, no solution bifurcates from the low temperature steady state, and it is impossible to ignite a low temperature steady state by increasing the liquid residence time. In such a case, the high temperature steady state can be attained only by preheating the reaction mixture. The presence of an isola thus may not be discovered in preliminary experiments, and its existence may lead to rather unexpected pitfalls in the operation of the reactor.

The occurrence of an isola may be better understood by examining Figure 4 which describes three Y_I graphs for

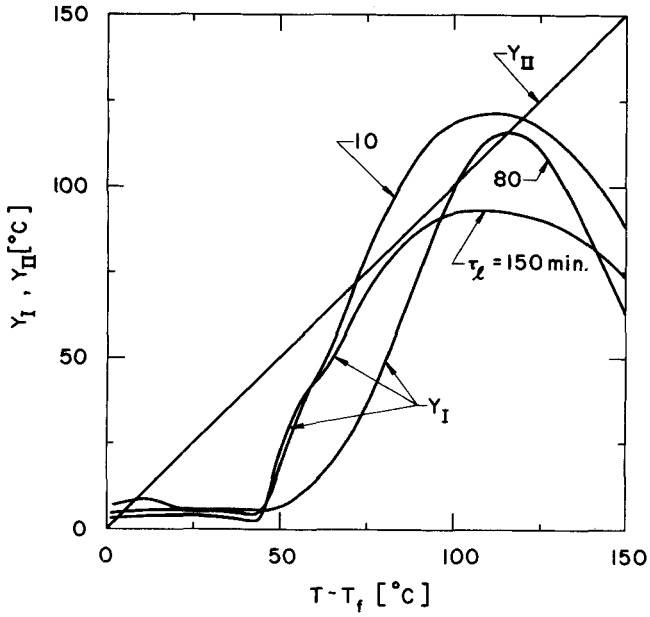

Fig. 4. The Y_I and Y_{II} graphs for case B of Figure 3.

TABLE 2. PARAMETERS USED FOR COMPUTING FIGURES 5 AND 6*

$T_f = 273°K$
$Ua = 0.1$ cal/(°K-s)
$k_l = 5\sqrt{D_A}$ cm/s
$\Delta H_s = 7\,000$ cal/mole
$\Delta E_2 = 45\,000$ cal/mole
$k_1\,(300°K) = 0.3$ cm^3/(mole-s)
$\lg_{10} P_B = 5.8613 - 4\,062/(1.8T - 144)$
$P_B = P_R = P_S$
$T_c = 273°K$
$a_v = 2$ cm^{-1}
$q_g = 2\,q_l$
$\Delta E_1 = 30\,000$ cal/mole
$k_1\,(525°K) = 50\,k_2\,(525°K)$

* All unspecified parameters have the same value as those in Table 1.

case B of Figure 3. The three Y_I curves have an inflection point. For the graphs corresponding to τ_l of 10 and 80 min., Y_I exceeds Y_{II} for some $T - T_f$ larger than that at which the inflection point occurs. However, this does not occur for the graph corresponding to τ_l of 150 min. In fact, the Y_I and Y_{II} graphs are tangent to each other for $\tau_l =$ 143 min., and for any higher liquid residence time a unique low temperature steady state exists.

The changes in k_1 have an interesting impact on the range of τ_l for which the steady state multiplicity occurs. A decrease of k_1 from 0.4 to 0.005 (curves C, B) causes a large increase in the range of τ_l for which multiplicity exists. However, a further decrease in k_1 causes a shrinking of this range until the isola completely disappears for $k_1 < 0.001$, yielding a unique low temperature steady state for all τ_l.

An analysis of steady state multiplicity of a CSTR in which a single exothermic second-order reaction is carried out revealed that up to five steady state solutions may be obtained (Hoffman et al., 1975). This is a rather unique feature of gas-liquid reactors, as no more than three steady state solutions can be attained in a single phase CSTR in which the same reaction is carried out.

When two consecutive reactions are carried out in a single phase CSTR, up to five steady state solutions can be obtained (Westerterp, 1962). Thus, by extrapolating from the single gas-liquid reaction case, it is conceivable that by adding a second consecutive reaction, whose rate is significant only at high temperatures, we can find cases for which up to seven steady state solutions exist. Numerical simulations verified this hypothesis. Table 2 reports the values of the parameters that were changed from

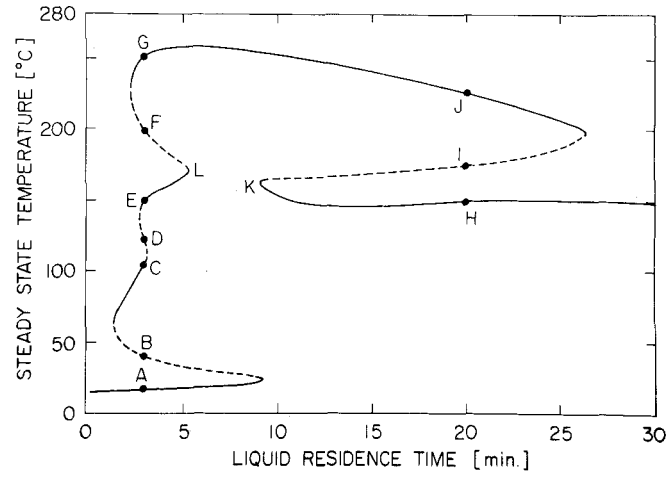

Fig. 5. Steady state multiplicity pattern for the example whose parameters are reported in Table 2.

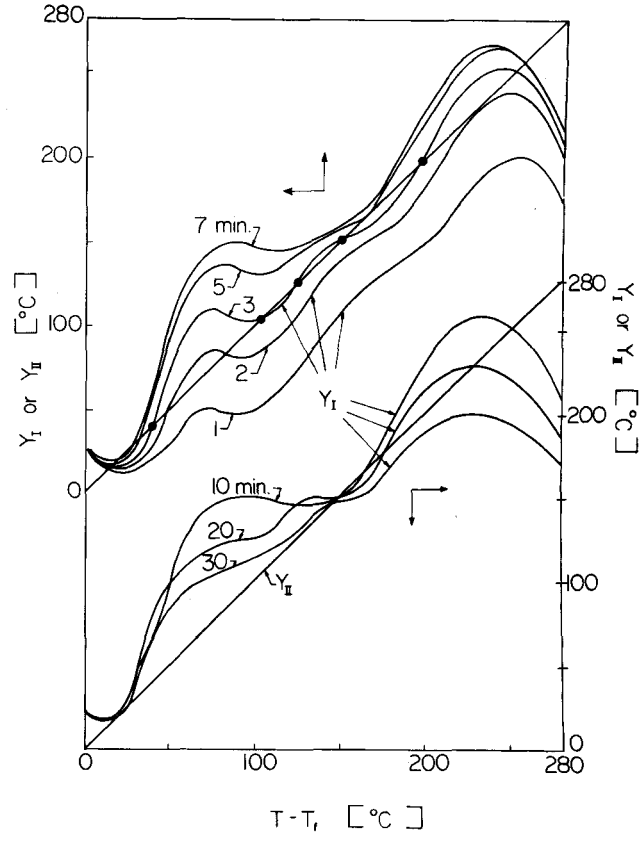

Fig. 6. The Y_I and Y_{II} graphs for the case whose parameters are reported in Table 2.

those reported in Table 1 in order to illustrate this unique behavioral feature of the system illustrated in Figures 5 and 6 for $\tau_l = 3$ min.

The multiplicity pattern for this system is rather intricate (Figure 5), and the system shifts continuously through regions of 1-3-5-7-5-3-1 solutions. These multiplicities are caused by the interactions among the rates of the chemical reactions, the rates of the transport phenomena, and the solubility of the gaseous reactant. The Y_I graphs corresponding to each multiplicity region are shown in Figure 6, and it is the change in the shape of these graphs that is responsible for the complex multiplicity pattern.

One of the interesting features of the system described in Figure 5 is that as the residence time is decreased along branch H-K, ignition to the branch G-J can occur. This feature is the inverse of the common ignition which is caused by an increase in the residence time.

TABLE 3. DATA FOR STEADY STATES MARKED IN FIGURE 5

Steady state	τ_l (min.)	T (°K)	Conversion of B	Selectivity†	M	E_A^*	E_B^*	E_R^*
A	3	289.6	0.01	1.00	0.003	0.09	0.004	0.004
B	3	313.6	0.18	1.00	0.02	0.19	0.13	0.13
C	3	377.5	0.56	1.00	0.91	1.25	1.25	1.25
D	3	396.5	0.67	1.00	2.04	2.00	2.00	2.00
E	3	423.6	0.84	0.99	4.82	3.71	3.69	3.67
F	3	470.4	0.91	0.79	20.8	9.26	7.66	6.06
G	3	528.4	0.93	0.29	113.1	50.98	29.81	8.62
H	20	422.5	0.997	0.81	0.63	1.08	0.92	0.75
I	20	448.5	0.992	0.64	3.00	1.95	1.44	0.92
J	20	503.9	0.987	0.18	23.7	13.57	7.45	1.32

† Selectivity is defined as moles of R formed per mole of converted B.

It is of interest to note that when the heat transfer coefficient for this example is increased, the bifurcation points K and L approach each other until an isola is formed. For high heat transfer coefficients, the high heat losses preclude the existence of very high steady state temperature. Therefore, further increases in the heat transfer coefficient cause the isola to shrink and finally to disappear. For the low temperature steady states, the rate of the second reaction is negligible, and the behavior is very similar to that of a reactor in which a single reaction occurs.

Table 3 reports predicted data for all the steady states corresponding to residence times of 3 to 20 min., respectively. (These steady states are marked in Figure 5). As expected, the higher the steady state temperature the higher is the conversion and the lower is the selectivity, where the selectivity is defined as the number of moles R formed per mole of converted B.

The table shows that for the seven steady states case, the Hatta number M changes from 0.003 for steady state A up to 113 for steady state G. These changes correspond to a change of the reaction factor E_A^* from 0.09 to 50.98 and are due to a shift from a chemical reaction to mass transfer control. This example clearly points out the need to account properly for the enhancement of the mass transfer rate by the chemical reaction in order to avoid pitfalls in predicting the rate of the heat generation and of the steady state temperature. The simple mass and chemical series resistances model used by Schmitz and Amundson (1963 *a* to *d*) is not adequate for describing such a system.

The design of gas-liquid reactors is usually based on a simplified model, as it is not possible at present to account in an exact quantitative fashion for all the physical and chemical rate processes as well as the mutual interactions among them. The simulations indicate that the multiplicity pattern as well as the ignition and extinction values are rather sensitive to the kinetic parameters. Consequently, the multiplicity can serve as an excellent test for the predictive capability of any model and as a means for discriminating among rival models and for estimation of kinetic parameters. To illustrate the point, consider graph B in Figure 3 which simulates our experiments with decane lot 3 (Figure 2 describes experimental data for this case). The simulation predicts an isola for $8.5 < \tau_l < 143$ min. We found in the experiments low temperature steady states for residence times up to 6 hr. (no experiments were performed for $\tau_l > 6$ hr.). Unfortunately, we did not consider at the time the possible existence of an isola and did not search for a high temperature steady state for $\tau_l > 143$ min. Clearly, such an experiment would have been most revealing about the validity of the model and the associated kinetic parameters.

The simulations also illustrate that the simple behavioral features of a single phase CSTR, in which a single chemical reaction occurs, cannot always be used to obtain a qualitative understanding of the multiplicity patterns of more complex reacting systems and reaction networks. It would be of definite interest to obtain an experimental proof of some of the complex multiplicity patterns predicted by our simulations.

NOTATION

a = exterior surface area of reactor
A = concentration of species A
a_l = dimensionless concentration, defined by (21)
a_v = interfacial area per unit volume
B = concentration of liquid reactant B
b_i = dimensionless concentration, defined by (20)
$\overline{b}$ = quantity defined by (20)
c_p = molar heat capacity
D = diffusion coefficient
ΔE = activation energy
E^* = reaction factor, defined by (4) to (6)
E_f = quantity defined by (22)
F = liquid volumetric flow rate
h = quantity defined by (18)
ΔH = heat of reaction
ΔH_s = heat of solubility
ΔH_v = heat of vaporization
k = reaction rate constant
k_l = mass transfer coefficient
M = Hatta number, defined by (18)
P = pressure in reactor
q = molar flow rate
Q = heat generation or removal functions, defined by (40)
R = reaction rate per unit volume of bulk and film liquid
r = dimensionless quantity, defined by (18)
r_i = dimensionless quantity, defined by (23)
s = dimensionless quantity, defined by (18)
T = temperature in reactor
T_c = exterior temperature of reactor
U = overall heat transfer coefficient
V_R = volume of reactor
x = mole fraction in liquid phase
Y = function defined by (41)
y = mole fraction in gas phase
z = coordinate normal to interface

Greek Letters

α = ratio of film to bulk volume, defined by (18)
γ = parameter defined by (18)
γ' = quantity defined by (19)

Γ_A = parameter defined by (24)
Γ_R = parameter defined by (25)
δ = thickness of liquid mass transfer film
ϵ = liquid holdup
θ = dimensionless residence time, defined by (18)
$\tilde{\rho}_l$ = molar density of liquid phase
τ = residence time

Subscripts

A = of species A
B = of species B
c = stream leaving condenser
f = feed stream
g = gaseous phase
i = gas-liquid interface
l = liquid phase
L = of species L
o = stream leaving reactor
R = of species R
S = of species S

LITERATURE CITED

Ding, J. S., Shanmuk Sharma, and Dan Luss, "Steady State Multiplicity and Control of the Chlorination of Liquid *n*-Decane in an Adiabatic Continuously Stirred Tank Reactor," *Ind. Eng. Chem. Fundamentals*, 13, 76 (1974).

Hoffman, L. A., M.S. thesis, "Theoretical Study of Steady State Multiplicity and Stability in Gas Liquid Continuous Stirred Tank Reactors," Univ. Houston, Tex. (1974).

———, Shanmuk Sharma, and Dan Luss, "Steady State Multiplicity of Adiabatic Gas-Liquid Reactors: 1. The Single Reaction Case," *AIChE J.*, 21, 318 (1975).

Pangarkar, V. G., "Gas Absorption With Reaction in a Solution Containing a Volatile Reactant," *Chem. Eng. Sci.*, 29, 877 (1974).

Schmitz, R. A., and N. R. Amundson, "An Analysis of Chemical Reactor Stability and Control—Two Phase Systems in Physical Equilibrium," *ibid.*, 18, 265 (1963*a*).

———, "An Analysis of Chemical Reactor Stability and Control—Two Phase Gas-Liquid and Concentrated Liquid-Liquid Reacting Systems in Physical Equilibrium," *ibid.*, 391 (1963*b*).

———, "An Analysis of Chemical Reactor Stability and Control—Two Phase Chemical Reacting Systems with Heat and Mass Transfer Resistances," *ibid.*, 415 (1963*c*).

———, "An Analysis of Chemical Reactor Stability and Control—Two Phase Chemical Reacting Systems with Fast Reactions," *ibid.*, 447 (1963*d*).

Szekely, J., and J. Bridgwater, "Some Further Consideration on Mass Transfer and Selectivity in Fluid-Fluid Systems," *ibid.*, 22, 711 (1967).

Teramoto, M., T. Nagayasu, T. Matsui, K. Hashimoto, and S. Nagata, "Selectivity of Consecutive Gas Liquid Reactions," *Chem. Eng. Japan*, 2, 186 (1969).

Van Krevelen, D. W., and P. J. Hoftijzer, "Kinetics of Gas Liquid Reactions—General Theory," *Rec. Trav. Chim. Pays-Bas*, 67, 563 (1948).

Westerterp, K. R., "Maximum Allowable Temperatures in Chemical Reactors," *Chem. Eng. Sci.*, 17, 423 (1962).

Manuscript received September 18, 1975; revision received and accepted September 28, 1975.

Mathematical Models of the Monolith Catalytic Converter:

LARRY C. YOUNG

and

BRUCE A. FINLAYSON

Department of Chemical Engineering
University of Washington
Seattle, Washington 98195

Part I. Development of Model and Application of Orthogonal Collocation

The orthogonal collocation method is applied to solve the mathematical model of a monolith catalytic converter, in which the reaction takes place in a porous catalytic layer deposited on the wall of a tube. A sequence of models is developed, with the most complicated one involving transient heat and mass transfer in three dimensions.

SCOPE

The orthogonal collocation method is developed for application to problems having irregular geometries. Most previous applications of orthogonal collocation in two dimensions have been for rectangular regions (Villadsen and Stewart, 1967; Sørensen et al., 1973; Young and Finlayson, 1973). A notable exception is the series of papers by Sørenson and Stewart (1974) dealing with flow of a fluid in a packed bed. In the applications to monolith catalytic reactors envisaged below, the duct frequently takes irregular shapes. Consequently, it is necessary to apply orthogonal collocation in these irregular three-dimensional geometries.

The monolith reactor is a large number of small, long tubes (in parallel) through which a gas flows, and catalyst is deposited on a porous layer on the wall of the duct. Another important objective is model discrimination; different mathematical models are developed for such devices in order to illustrate the phenomena oc-